PERGAMON

Micron 33 (2002) 483–487

micron

www.elsevier.com/locate/micron

Electron tomography and computer visualisation of a three-dimensional 'photonic' crystal in a butterfly wing-scale

A. Argyros[a,*], S. Manos[b], M.C.J. Large[a], D.R. McKenzie[c,a], G.C. Cox[c,d], D.M. Dwarte[d]

[a]*School of Physics, University of Sydney, Sydney, NSW 2006, Australia*
[b]*Sydney Vislab, University of Sydney, Sydney, NSW 2006, Australia*
[c]*Key Centre for Microscopy and Microanalysis, University of Sydney, Sydney, NSW 2006, Australia*
[d]*Electron Microscope Unit, University of Sydney, Sydney, NSW 2006, Australia*

Received 28 March 2001; revised 18 June 2001; accepted 26 August 2001

Abstract

A combination of transmission electron tomography and computer modelling has been used to determine the three-dimensional structure of the photonic crystals found in the wing-scales of the Kaiser-I-Hind butterfly (*Teinopalpus imperialis*). These scales presented challenges for electron microscopy because the periodicity of the structure was comparable to the thickness of a section and because of the complex connectivity of the object. The structure obtained has been confirmed by taking slices of the three-dimensional computer model constructed from the tomography and comparing these with transmission electron microscope (TEM) images of microtomed sections of the actual scale. The crystal was found to have chiral tetrahedral repeating units packed in a triclinic lattice.

Keywords: Tomography; Naturally occurring chiral photonic crystal; *Teinopalpus imperialis*; Visualisation

1. Introduction

There are many structures in nature that cannot be easily solved in three dimensions through conventional scanning electron microscope (SEM) and transmission electron microscope (TEM) microscopy. This is especially true of repeated or crystalline structures, which lie in a size range where each repeating unit is larger than the convenient thickness of a section. In such cases there is difficulty in determining the three-dimensional connectivity of the structure.

By acquiring a series of TEM images at a range of tilt angles, tomography methods can be used to reassemble these images into a three-dimensional object. The application of electron tomography to relatively simple (non-repeating or repeating but non-crystalline) structures has already been demonstrated (e.g. Martone et al., 2000; Moritz et al., 1995; Nicastro et al., 2000; Taylor et al., 1999). One study has recently reported using electron tomography to characterise a naturally occurring crystalline membrane structure (Deng et al., 1999). However, even tomography was not able to fully determine the structure.

Here we report on the application of electron tomography and a powerful computer modelling technique to completely solving a well-defined naturally occurring crystalline structure in the wing-scales of the Kaiser-I-Hind butterfly (*Teinopalpus imperialis*) (Ghiradella, 1994). This structure is particularly challenging because it occurs in the problematic size range and it has complex connectivity. It is also a good subject for study as it is an excellent example of a naturally occurring three-dimensional photonic crystal. The periodic structure under some conditions can impede the propagation of light within a wavelength range in certain directions in the structure leading to strong reflection of the light in this range. In this respect the phenomenon is related to the development of a band gap for electron wave propagation in semiconductors. Such crystals are under active study because of their interesting light scattering properties (Yablanovitch, 1993). These particular crystals are essentially three-dimensional lattices made from the structural protein chitin, a naturally occurring polymer similar in structure to cellulose. They have previously been reported though their structure has not been determined (Vikusic, 2000).

2. Methods used

In preliminary studies of the scales, a single scale

* Corresponding author. Present address: Optical Fibre Technology Centre, 206 National Innovation Centre, Australian Technology Park, Eveleigh, NSW 1430, Australia. Tel.: +61-2-935-1-1930; fax: +61-2-935-1-1911.

E-mail address: a.argyros@oftc.usyo.edu.au (A. Argyros).

0968–4328/02/$ - see front matter
PII: S0968-4328(01)00044-0

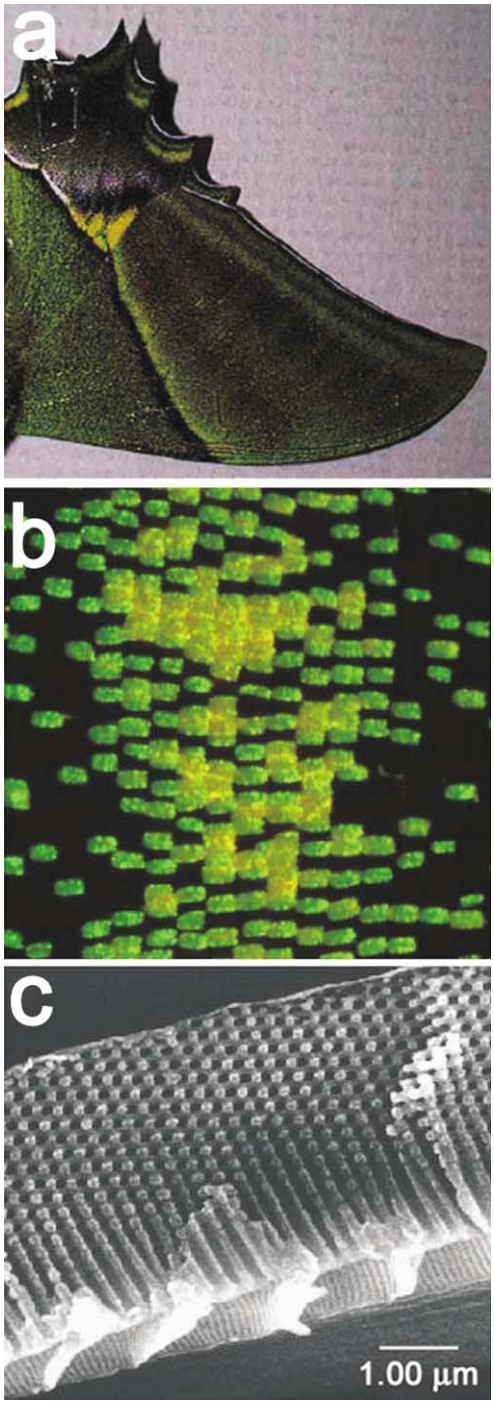

Fig. 1. (a) The wing of the Kaiser-I-Hind butterfly. (b) Optical microscope image showing the scales on the wing, the black ground scales and the green cover scales containing the photonic crystals. (c) SEM image of a cross section of one of the green scales showing the periodic structure.

was prepared by cutting with a blade and viewed edge-on in a SEM (Fig. 1). The SEM images indicated that the structure was periodic with a repeat distance in the order of 300 nm whilst the structure had features as small as 60 nm. Such SEM images alone could not solve the structure as the fracture occurs along planes of weakness, marked by the narrowest parts of the lattice and the inner parts of the structure are obscured from view.

The wing scale was viewed in cross section in the TEM. The structure was clearly visible and two important features became apparent. First, the appearance of the structure is strongly dependant on the position and orientation of the plane of the section. Second, there are many regions in which a discontinuous change of orientation occurs across a line, very similar to the effect of a grain boundary in polycrystalline specimens. The typical size of a single crystalline region was 30–40 periods.

Serial TEM sectioning is a possible means for obtaining further information, but according to the Nyquist Sampling Theorem, in order to resolve the smaller features, a sampling frequency of at least twice the spatial frequency of the features is required. Thus, to solve the structure would require at least twenty sections of the order of 30 nm, a tedious and difficult task given that the sections need to be imaged with minimum distortion and brought into registration. Sections of 90 nm thickness were imaged and it was found that some exhibited tearing, folding and drifting, indicating that 30 nm sections would require a substantial improvement in embedding and sectioning techniques. A tomographic approach would overcome the limitations of TEM and SEM as it would allow for the three-dimensional structure of each section to be determined.

2.1. Transmission electron tomography

We employed a tomographic technique which involves taking TEM images of the sample from different directions by rotating the sample; this set of images forms the tilt series. From this series, a set of images was generated representing a series of adjacent slices through the sample. This new set of images allows the sample to be reconstructed in three dimensions (to give the tomogram). The software used to complete the tomography and create the first draft model was IMOD (Kermer et al., 1996).

Tomography was performed on three sections of different thickness, namely 100, 200 and 500 nm. It was expected that the 100 and 200 nm sections would not completely solve the structure, due simply to the fact that the periodicity was about 300 nm, but the tomography was completed none the less and models for the structure obtained. The two sections were taken in perpendicular directions thus they could be combined to give enough information to characterise the entire lattice. The 100 nm section, unlike the 90 nm sections, was imaged easily and showed no signs of structural instability.

A 500 nm section would be useful to view as it would give information about a substantial portion of the structure, however, it was feared that for such a thick specimen chromatic aberration would give an unsharp image and penetration by electrons may not be adequate. However, the open nature of the crystal meant that penetration was adequate and the images were sufficiently sharp for the resolution

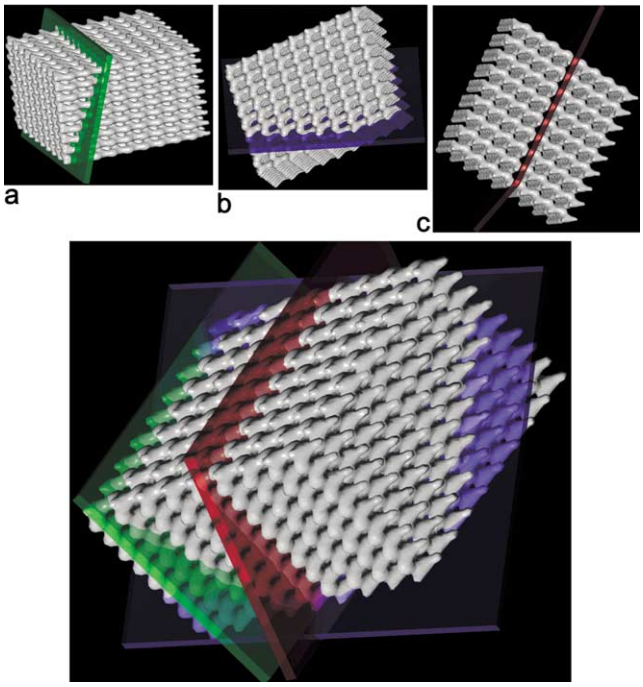

Fig. 2. The three-dimensional-model of the crystal structure constructed in the three-dimensional-animation software Houdini. In the top three sections a, b and c, the coloured slices of 90 nm thickness indicate the slice that was cut out of the model to produce the artificial TEM images shown in Fig. 3.

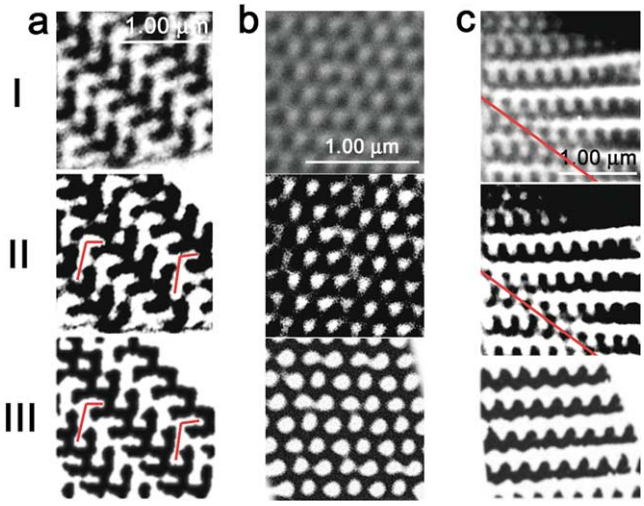

Fig. 3. The columns a, b and c show TEM images of the crystal in three different orientations corresponding to the slices in Fig. 2a–c, respectively. Row I shows the real TEM image of each slice. Row II shows the contrast enhanced real TEM images, showing how the real TEM images would look if the material of the crystal was completely opaque. Row III shows the artificial TEM images obtained by slicing the Houdini model as in Fig. 2 and treating the material as completely opaque. Several features of the images have been traced out in a(II) and the lines that trace these features have been superimposed onto a(III). The agreement between the row II and row III images indicated that the model was correct. The actual appearance of the real and simulated images is very sensitive to the position and orientation of the sectioning plane and small point to point variations seen in both real and simulated images are caused by the sectioning plane being not strictly related to the symmetry planes and axes of the structure. An example of the grain boundaries discussed in the text is seen in images (c)(I) and (c)(II) as a line of discontinuity in the image. Grain boundaries were not included in the computer model.

required. The model constructed from the 500 nm section tomogram was in agreement with that constructed from the 100 and 200 nm tomograms and allowed for the dimensions of the lattice to be calculated more accurately as well as the connectivity and topology of the lattice to be finalised.

2.2. Computer visualisation

The software used for the tomography allows the Cartesian coordinates of points in the model to be read. The coordinates were put into three-dimensional-animation software and the model for the structure was reconstructed there. The three-dimensional-animation software used for the computer modelling was Sidefx Software's Houdini (http://www.sidefx.com). Houdini allowed the model to be extended thus many unit cells could be created from the coordinates of just one (these being the average of all the unit cells directly measured from the tomograms), allowing for a model of a large lattice to be generated.

The computer model was sliced to obtain 'artificial' TEM images—many different images could be obtained by changing the orientation of the slicing plane. These computer generated TEM images could then be compared to the real TEM images obtained earlier from the 90 nm thick sections. The artificial TEM images were obtained by either treating the solid parts of the model as completely opaque and adjusting the levels on the real TEM images to simulate this, or by adjusting the transparency of the model to match the transparency of the real structure. The large chitin structures act as electron absorbing objects and hence the contrast of the image was not sensitive to focus, as would occur in weakly absorbing structures acting as phase objects. The interpretation of these is therefore much more straightforward than for atomic level periodic objects.

The computer model could be readily manipulated to allow the structure to be visualised more clearly (Fig. 2). It also acted as a verification tool, by allowing the artificial TEMs to be compared with the real TEM sections obtained using conventional TEM (Fig. 3). This proved to be a particularly valuable aid in resolving issues such as the connectivity of the structure, which was not obvious from the tomography.

2.3. Technical notes on transmission electron microscopy

To prepare the samples for TEM a wing-scale was treated for one hour with a primary fix (2.5% glutaraldehyde in 0.1 M phosphate buffer and a trace of detergent) and for one hour in a secondary fix (1% Osmium tetroxide in 0.1 M phosphate buffer). The scale was then dehydrated in a graded series of alcohol, infiltrated in Spurrs Resin and left to dehydrate at 60 °C. The scale was sectioned using an ultramicrotome and the sections picked up on copper

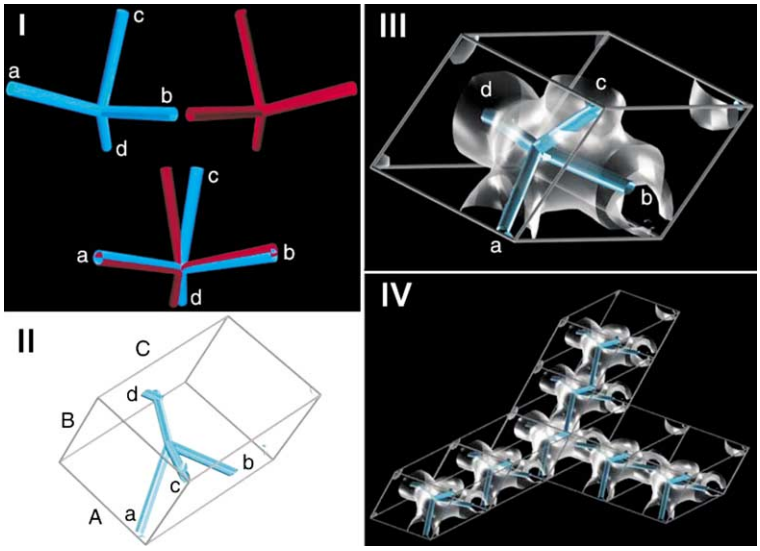

Fig. 4. I (top) The skeleton of the fundamental tetrahedral unit is shown on the left with its reflection shown on the right. (bottom) The two cannot be superimposed, thus showing that the tetrahedron is chiral. II The primitive triclinic cell with the skeleton of the tetrahedron inside it. III The primitive cell with the tetrahedron having a skin around it to indicate its true thickness. IV Several unit cells indicating how the primitive cells stack to form the entire lattice. All dimensions are given in Table 1.

grids. The microscope used for the tomography and TEM imaging was a Phillips Biofilter CM120 TEM operating at 120 kV. The images were captured on a Gatan Slow Scan cooled ccd camera. For the 100 and 500 nm sections the tilt series was over a 70° range with 2.5° increments and for the 200 nm section it was over a 120° range with 2.5° increments, all three being about a single axis. The magnification used limited the pixel size to approximately 7 nm; the tomogram consisted of 7 nm thick z-slices, thin enough to completely solve the structure and impossible to obtain by physically slicing the scale.

3. Results

From the SEM images (shown in Fig. 1) we deduced that the structure has a tetrahedral object as the repeat unit. However, the connectivity could not be determined from the external topographic information alone.

Tomography on the 100 and 200 nm sections confirmed that the structure has a tetrahedral repeating unit and allowed the dimensions and symmetry of the repeat unit to be directly measured. Because the sections were thinner than the 300 nm periodicity of the lattice, the three-dimensional connectivity of the tetrahedra could not be determined unambiguously from these tomograms.

Tomography of a 500 nm section, thicker than the periodicity of the lattice, was carried out and allowed the connectivity to be determined. This information was entered into Houdini to finalise the computer model. Artificial TEM images obtained by taking slices from this final model agreed sufficiently well with the real TEM images to validate the model for the structure (Fig. 3). A similar method to confirming a model produced from a tomogram has been used in the past (Deng et al., 1999), however the comparison then was between infinitesimal slices of the tomogram itself and a mathematical model for the structure. Our case is a direct comparison between real TEM images and finite-thickness slices of the model. This comparison confirmed features of the structure such as the connectivity.

A difficulty associated with obtaining the artificial TEM images of slices of the computer model is that there are essentially an infinite number of ways the model can be sliced. Having a large lattice meant that different slices, whose orientations and positions in the lattice are very close, can nevertheless produce vastly different results. A large number of real and artificial sections were studied. We concentrated on a number of patterns that looked unusually ‘complicated’ in real sections, and then looked to see if these patterns appeared in the artificial TEM sections. An example of these structures is shown in Fig. 3a(II). This appears to show a ‘doublet’ structure, which is not an obvious cross section of a lattice made of tetrahedral units. However, the same pattern was obtained in artificial TEM’s (Fig. 3a(III)). The ability to reproduce all of the ‘complicated’ patterns shows that the model is correct.

The model for the photonic crystal (Fig. 4 and Table 1) is a triclinic lattice where the repeat unit is a distorted tetrahedron. The tetrahedron and its mirror image are compared in Fig. 4(I). The mirror image cannot be rotated onto the original object, a property referred to as ‘chirality’. The four arms of the chiral tetrahedron in one cell meet the arms of neighbouring tetrahedra. However, one pair of faces of the triclinic cell has none of the arms passing through it. In this way the four fold coordination of the tetrahedron is consistent with the six nearest neighbours of the unit cell.

Table 1
The dimensions of the tetrahedral unit and the triclinic primitive cell are presented, the labels are as in Fig. 4. The thickness of each arm of the tetrahedron (indicated in Fig. 4(III)) is around 100 nm but varies

Dimensions of tetrahedron				Dimensions of triclinic primitive cell			
Lengths (nm)		Angles between arms		Lengths (nm)		Acute angles between sides	
a	190 ± 31	ab	86° ± 9°	A	267 ± 24	AB	79° ± 8°
b	190 ± 15	ac	72° ± 12°	B	212 ± 26	AC	64° ± 7°
c	190 ± 32	ad	135° ± 9°	C	325 ± 24	BC	84° ± 8°
d	130 ± 19	bc	59° ± 8°				
		bd	128° ± 12°				
		cd	145° ± 14°				

4. Conclusions

We have found that electron tomography, combined with computer based visualisation, is a successful strategy for determining three-dimensional structures with a characteristic size in the submicrometre range. The periodicity of the photonic crystal in the wing-scales of *Teinopalpus imperialis* provided special challenges because it was comparable to the specimen thickness. A key test of a successful structure determination was the comparison of slices taken from the three-dimensional computer model with images of real sections taken with the TEM.

Acknowledgements

The authors would like to thank Anne S. Gomes for the sample preparation and Ben Simons for his assistance with the three-dimensional-modelling.

References

Deng, Y.R., Marko, M., Buttle, K.F., Leith, A., Mieczkowski, M., Mannella, C.A., 1999. Cubic membrane structures in amoeba (*Chaos carolinensis*) mitochondria determined by electron microscopic tomography. Journal of Structural Biology 127 (3), 231–239.

Ghiradella, H., 1994. Structure of butterfly scales—patterning in an insect cuticle. Microscopy Research and Technique 27, 429–438.

Kermer, J.R., Mastronarde, D.N., McIntosh, J.R., 1996. Computer visualisation of three-dimensional image data using IMOD. Journal of Structural Biology 116, 71–76.

Martone, M.E., Deerinck, T.J., Yamada, N., Bushong, E., Ellisman, M.H., 2000. Correlated three-dimensional light and electron microscopy: Use of high voltage electron microscopy and electron tomography for imaging large biological structures. Journal of Histotechnology 23 (3), 261–270.

Moritz, M., Braunfeld, M.B., Sedat, J.W., Alberts, B., Agard, D.A., 1995. Microtubule nucleation by γ-tubulin-containing rings in the centrosome. Nature 387, 638.

Nicastro, D., Frangakis, A.S., Typke, D., Baumeister, W., 2000. Cryo-electron tomography of Neurospora mitochondria. Journal of Structural Biology 129 (1), 48–56.

Taylor, K.A., Schmitz, H., Reedy, M.C., Goldman, Y.E., Franzini-Armstrong, C., Sasaki, H., Tregear, R.T., Poole, K., Lucaveche, C., Edwards, R.J., Chen, L.F., Winkler, H., Reedy, M.K., 1999. Tomographic three-dimensional reconstruction of quick-frozen, Ca2 + -activated contracting insect flight muscle. Cell 99 (4), 421–431.

Vikusic, P., Sambles, J.R., Ghiradella, H., 2000. Optical classification of microstructures in butterfly wing-scales. Photonic Science News 6 (1,2), 61–66.

Yablanovitch, E., 1993. Photonic band-gap structures. Journal of the Optical Society of America 10 (2), 283.